Identification of Adenosine Functional Groups Involved in Substrate Binding by the Ribonuclease P Ribozyme†

Darrick Siew,‡,§ Nathan H. Zahler,‡ Adam G. Cassano,‡ Scott A. Strobel,|| and Michael E. Harris*,‡

Department of Molecular Biology and Microbiology, Case Western Reserve University School of Medicine, Cleveland, Ohio 44106, and Department of Molecular Biophysics and Biochemistry, Yale University School of Medicine, New Haven, Connecticut 06520

Received September 29, 1998; Revised Manuscript Received November 23, 1998

ABSTRACT: The RNA component of bacterial ribonuclease P (RNase P) binds to substrate pre-tRNAs with high affinity and catalyzes site-specific phosphodiester bond hydrolysis to generate the mature tRNA 5′ end. Herein we describe the use of biotinylated pre-tRNA substrates to isolate RNase P ribozyme−substrate complexes for nucleotide analogue interference mapping of ribozyme base functional groups involved in substrate recognition. By using a series of adenosine base analogues tagged with phosphorothioate substitutions, we identify specific chemical groups involved in substrate binding. Only 10 adenosines in the *Escherichia coli* ribozyme show significant sensitivity to interference: A65, A66, A136, A232−234, A248, A249, A334, and A347. Most of these adenosine positions are universally conserved among all bacterial RNase P RNAs; however, not all conserved adenosines are sensitive to analogue substitution. Importantly, all but one of the sensitive nucleotides are located at positions of intermolecular cross-linking between the ribozyme and the substrate. One site of interference that did not correlate with available structural data involved A136 in J11/12. To confirm the generality of the results, we repeated the interference analysis of J11/12 in the *Bacillus subtilis* RNase P ribozyme, which differs significantly in overall secondary structure. Notably, the *B. subtilis* ribozyme shows an identical interference pattern at the position (A191) that is homologous to A136. Furthermore, mutation of A136 in the *E. coli* ribozyme gives rise to a measurable increase in the equilibrium binding constant for the ribozyme-substrate interaction, while mutation of a nearby conserved nucleotide (A132) that is not sensitive to analogue incorporation does not. These results strongly support direct participation of nucleotides in the P4, P11, J5/15, and J18/2 regions of ribozyme structure in pre-tRNA binding and implicate an additional region, J11/12, as involved in substrate recognition. In aggregate, the interference results provide a detailed chemical picture of how the conserved nucleotides adjacent to the pre-tRNA substrate contribute to substrate binding and provide a framework for subsequent identification of the specific roles of these chemical groups in substrate recognition.

Ribonuclease P is a widespread tRNA-processing endonuclease that catalyzes formation of the mature tRNA 5′ end. RNase P enzymes generally are ribonucleoproteins, and the RNA subunits spanning all three phylogenetic domains share significant sequence and structural homology (*1*, *2*). Bacterial RNase P is a heterodimer composed of a single large RNA subunit (ca. 400 nucleotides) and a smaller protein subunit (ca. 100 amino acids). The RNA alone can catalyze the cleavage reaction in vitro in the presence of divalent metal ions; thus, bacterial RNase P RNAs form one class of RNA enzymes, or ribozymes (*3*; reviewed in *4*).

Substrate recognition is an essential component of enzyme function. RNase P ribozymes bind substrate pre-tRNA with high affinity as reflected in a dissociation constant of 35−100 nM (e.g., refs *5* and *6*). Significant effort has been invested in defining tRNA sequences and structures required for recognition by the ribozyme. Deletion and chemical-protection experiments show that most of the determinants required for tRNA 5′ end formation by RNase P are located in the acceptor stem and the T-stem and loop (e.g., refs *7*−*10*). Mutagenesis and chemical interference studies identified substrate nucleotides and functional groups in this region that are important for binding (*12*−*15*), including 2′ hydroxyl groups at positions 53, 54, 61, and 62 (*16*) and phosphate oxygens at positions 56, 59, and 61 (*12*). tRNA nucleotide bases recognized by RNase P RNA include the 3′ CCA sequence (*10*), the G1-C72 base pair at the cleavage site (*11*), and cytosine N4 of the C56-G19 pairing between the T- and D-loops (*16*). However, in many cases, the specific interactions in which these functional groups participate remain to be defined.

† This work was supported by NIH Grant GM56740 to M.E.H. and an NSF Career award (CHE-9701787) to S.A.S. and by a Howard Hughes Medical Institute grant to Case Western Reserve University School of Medicine. A.G.C. is the recipient of a graduate fellowship from the HHMI.

* Corresponding author: Phone (216) 368-4779; FAX (216) 368-3055; email meh2@pop.cwru.edu.

‡ Case Western Reserve University School of Medicine.

§ Present address: College of Medicine and Public Health, Ohio State University, Columbus, OH 43210.

|| Yale University School of Medicine.

10.1021/bi982329r CCC: $18.00
Published on Web 01/20/1999

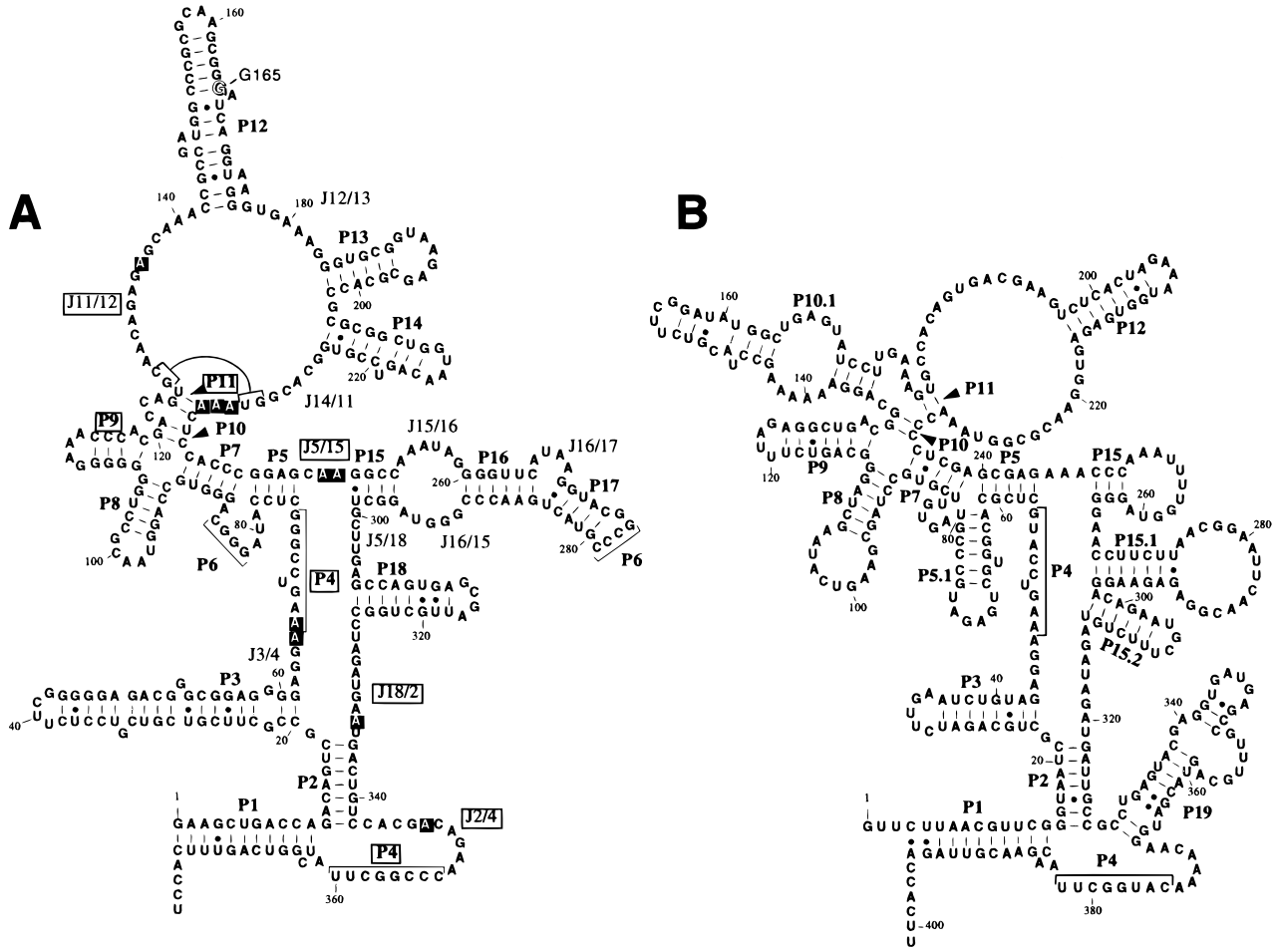

FIGURE 1: Secondary structure of (A) *E. coli* RNase P RNA and (B) *B. subtilis* RNase P RNA. Helices are numbered from the 5′ end and given the designation P (paired). Regions joining helices are given the designation J (joining) and numbered according to the helices that they connect [i.e., J3/4 connects helices P3 and P4 (*17*)]. Nucleotides forming helices P4 and P6 are indicated with brackets. Regions of the secondary structure referred to in the text are boxed. The position of the 5′ end of the Ec165 circularly permuted ribozyme is highlighted. Adenosine positions sensitive to analogue incorporation are shown in black boxes.

Two specific contacts between the ribozyme and substrate RNAs have been identified. First, the internal bulge adjacent to helix P15 (nomenclature from ref *17*; see Figure 1) in RNase P RNA is the binding site for the 3′-terminal pre-tRNA CCA sequence (*10, 18, 19*). Part of the CCA docking interaction involves pairing between the pre-tRNA C residues at positions +74 and +75 and nucleotides G292 and G293 in *Escherichia coli* RNase P RNA (*10*). A second ribozyme−substrate interaction detected by Pan and co-workers involves hydrogen bonding between the 2′ hydroxyl at tRNA position 60 and N1 of A230 in *Bacillus subtilis* RNase P RNA (*15, 16*).

Additional sites of contact between the ribozyme and substrate have been implicated by positioning photoaffinity cross-linking reagents at specific sites in both the ribozyme and substrate. Intermolecular cross-linking indicates that J5/15 and J18/2 are in close proximity to the acceptor stem and the 5′ leader sequence of the pre-tRNA substrate (Figure 1; *20*−*22*, *44*). However, specific contacts between J18/2 or J5/15 and the substrate have not been defined. Also, photoagents at positions 52 and 64 in the T-stem of tRNA detect nucleotides in P9 and P11 of the ribozyme (*23*), and several nucleotides in P9 and P11 are protected from chemical modification by substrate or, when mutated, result in decreased affinity for pre-tRNA (*16, 18*). Thus, an important goal is identification of specific essential functional groups in J5/15, J18/2, P9, and P11 and characterization of the interactions of these moieties with pre-tRNA.

Nucleotide analogue interference mapping (NAIM) utilizes specific nucleotide analogues for modification−interference to identify functional groups essential for RNA activity (*24*). Nucleotide analogues that contain alterations of single functional groups are covalently tagged with a 5′ phosphorothioate linkage and randomly incorporated into RNAs by in vitro transcription. The RNAs are then separated into active and inactive populations on the basis of their ability to perform a specific function. Positions of analogue incorporation are determined by chemical cleavage at the phosphorothioate linkage (*25*). Interference by analogue incorporation at a specific nucleotide results in underrepresentation of modification at that site in the active population. This approach has been used to define the chemical basis for nucleotide sequence conservation in the group I intron (*26*) and to define how the substrate is docked into the active site of that catalytic RNA (*27*). The same approach could be used to identify the tertiary interactions responsible for substrate binding in the RNase P ribozyme.

Modification−interference approaches rely on the ability to separate active from inactive molecules in mixed populations of modified RNAs. Native RNase P RNA, unlike other ribozymes, reacts in an intermolecular fashion. Hartmann and colleagues have used a gel-mobility shift approach to separate

enzyme−product complexes from free enzyme in order to identify phosphate and 2′-hydroxyl groups in the ribozyme that, when modified with 2′-deoxy or phosphorothioate derivatives, interfere with substrate binding (*28*, *29*). Sensitive backbone positions are distributed throughout the ribozyme in both conserved and phylogenetically variable regions. A number of sites sensitive to phosphorothioate and deoxyphosphorothioate substitution are located in known elements of tertiary structure (e.g., GNRA tetraloop interactions) and thus indicate areas where functional group modification had an indirect effect on substrate binding. Although interference due to structural perturbation is of significant interest, this phenomenon complicates interpretation of the results with respect to identification of individual contact points between the ribozyme and substrate.

To build upon the previous interference analysis, we developed an interference system that could suppress effects due to minor structural perturbation and also permit selection under a broad range of reaction conditions and ribozyme−substrate concentrations. We find that RNase P ribozymes bind to biotinylated pre-tRNA substrates immobilized on streptavidin−agarose beads with an equilibrium binding constant that is similar to that for the native ribozyme and substrate in vitro. This system was applied in NAIM analysis to identify individual adenosine functional groups that are involved in substrate binding. Nucleotides sensitive to analogue incorporation are largely located at nucleotide positions conserved in bacterial RNase P RNAs, and a subset are conserved among RNase P RNAs from all three phylogenetic domains. Further investigation of one of the sensitive adenosine nucleotides demonstrates the generality of the interference results for bacterial RNase P ribozymes and the relevance of the interference data for ribozyme function.

MATERIALS AND METHODS

Preparation of RNA. RNase P RNAs from *E. coli* and *B. subtilis* and pre-tRNA^{Asp} from *B. subtilis* were generated by in vitro transcription from linearized plasmid DNA templates with T7 RNA polymerase. *E. coli* RNase P RNA was transcribed from pDW98 digested with the restriction enzyme *Sna*BI, *B. subtilis* RNase P RNA was transcribed from pDW66 digested with *Dra*I, and pre-tRNA^{Asp} was transcribed from pDW152 digested with *Bst*NI. All three plasmids were generous gifts from the laboratory of Dr. Norman R. Pace. RNA transcription reactions were generally performed at a volume of 100 μL and contained 1 mM NTPs, 40 mM Tris-HCl, pH 7.9, 6 mM magnesium chloride, 2 mM spermidine, and 10 mM dithiothreitol and were incubated at 37 °C for 10−14 h. To facilitate subsequent 5′ end-labeling, guanosine was included in transcription reactions at a concentration of 5 mM. For uniform labeling of the RNA, 20 μL transcription reactions were carried out essentially as described above, but they contained 50 μCi of [α-^{32}P]GTP [300 Ci/mmol (NEN)]. To generate biotinylated pre-tRNA, bio-11-UTP [5-[*N*-(*N*-biotinyl-ϵ-aminocaproyl)-3-aminoallyl]uridine 5′-triphosphate (Sigma)] was included in the transcription reaction at a concentration of 0.5 mM and the unmodified UTP concentration was maintained at 1 mM. Reactions were terminated by dilution to 200 μL with 10 mM Tris-HCl, pH 8.0, and 1 mM EDTA and addition of sodium acetate to 0.3 M followed by extraction with phenol and chloroform. The resulting RNA products were ethanol-precipitated and purified by polyacrylamide gel electrophoresis. Full-length RNA products were visualized by UV shadowing and the RNA bands were excised from the gel. RNAs were eluted by incubating the gel slice in 4 volumes of 40 mM Tris-HCl, pH 8.0, 1 mM EDTA, 0.3 M sodium acetate, and 0.1% sodium dodecyl sulfate for 4−12 h. Eluted RNAs were extracted with phenol and chloroform and recovered by ethanol precipitation. The amount of RNA obtained was determined by measuring absorbance at 260 nm.

The 5′-*O*-(1−thio)nucleoside triphosphate derivatives of 2,6-diaminopurine riboside (DAPαS), 2-aminopurine riboside (2APαS), purine riboside (PurαS), N^6-methyladenosine (^{NMe}AαS), and N^7-deazaadenosine (7dAαS) were synthesized as described (*24*, *26*). Incorporation of the analogues into RNase P RNA at a level of approximately 5% by in vitro transcription was achieved by normalizing the amount of observed iodine cleavage of end-labeled transcription products to that of adenosine phosphorothioate-modified controls (by using 50 μM S$_P$-ATPαS). The following nucleotide concentrations were found to be optimal for analogue incorporation into *E. coli* and *B. subtilis* RNase P RNAs by in vitro transcription: 0.1 mM DAPαS and 1 mM ATP; 0.25 mM 2APαS and 1 mM ATP; 0.25 mM PurαS and 1 mM ATP; 0.25 mM ^{NMe}AαS and 0.5 mM ATP; or 0.25 mM 7dAαS and 0.5 mM ATP.

Isolation of E−S Complexes Using Biotinylated Pre-tRNA. For separation of E−S complexes from unbound ribozyme, up to 3 μg of guanosine-primed RNase P RNA was 5′ end-labeled with T4 polynucleotide kinase in a 20 μL reaction containing 20 mM Tris-HCl, pH 7.5, 5 mM magnesium chloride, 1 mM dithiothreitol, 100 mM sodium chloride, and 250 μCi of [γ-^{32}P]ATP [6000Ci/mmol (NEN)]. Labeled RNAs were gel-purified and recovered by ethanol precipitation. RNAs were renatured by incubation at 65 °C for 90 s followed by incubation at 37 °C for 15 min. Biotinylated substrate pre-tRNA in 10 mM Tris-HCl, pH 8.0, and 1 mM EDTA was added after renaturation to concentrations from 1 nM to 1.5 μM. The substrate and ribozyme RNAs were incubated together for 5 min at 37 °C in binding reaction buffer (1 M ammonium acetate, 40 mM Tris-HCl, pH 8.0, 25 mM calcium chloride, and 0.01% NP-40) before addition to preblocked streptavidin−agarose beads (Sigma). No increase in the bound fraction was detected when binding reactions were incubated for times longer than 5 min, indicating that the reactions had come to equilibrium (data not shown). Nonspecific binding sites in the beads were blocked by incubating 50 μL of beads with 400 μL of a solution containing 25 μg/mL glycogen, 20 μg/mL BSA, 10 μg/mL poly(A) RNA, 50 mM Tris-HCl, pH 8.0, 100 mM sodium chloride, and 0.01% NP-40. Beads were then washed twice with 400 μL of 50 mM Tris-HCl, pH 8.0, 100 mM sodium chloride, 0.01% NP-40, and twice with 400 μL of 1 M ammonium acetate, 40 mM Tris-HCl, pH 8.0, 25 mM calcium chloride, and 0.01% NP-40. Ribozyme−substrate binding reactions were incubated with preblocked beads for 2 min at room temperature. Beads were pelleted by brief (ca. 7 s) centrifugation. The resulting free ribozyme in the supernatant was recovered by ethanol precipitation. The beads were washed two times with 200 μL of binding assay buffer for 10 s. Longer wash times significantly reduced the amount of ribozyme recovered (data not shown). The bound material was eluted by incubating the beads for 10 min at

85 °C in 200 μL of 40 mM Tris-HCl, pH 8.0, 1 mM EDTA, 0.3 M sodium acetate, and 0.1% sodium dodecyl sulfate. RNAs in the bound and unbound fractions were recovered by phenol extraction and ethanol precipitation. Dissociation constants (K_d) were measured by binding uniformly radiolabeled RNase P RNA at concentrations 5−10-fold below the concentration of substrate to the immobilized biotinylated pre-tRNA and measuring the fraction bound by scintillation counting. These data were fit to (*30*)

$$[E-S]/[E-S]_\infty = 1/(1 + (K_d/[S])) \quad (1a)$$

where [E−S] is the amount of radioactivity recovered in the bound fraction, $[E-S]_\infty$ is the maximal amount of bound radioactivity recovered, and [S] is the concentration of biotinylated substrate in the binding reaction.

Single Turnover and Binding Kinetics. The apparent cleavage rate (k_{app}) for a single-turnover reaction under conditions of excess enzyme ([E]/[S] > 5) was performed at pH 6.0 in order to suppress the cleavage rate so that time points could be collected manually (*31*). RNase P RNA and uniformly labeled pre-$tRNA^{Asp}$ were incubated separately in 1 M sodium chloride and 40 mM PIPES, pH 6.0, and heated to 95 °C for 1 min, followed by addition of magnesium chloride to 25 mM and further incubation at 37 °C for 15 min. Reactions (20 μL) were initiated by mixing ribozyme and substrate and incubated at 37 °C. Aliquots (2 μL) of the reaction were taken at times ranging from 6 s to 20 min and cleavage was terminated by addition of EDTA to 100 mM. Reaction products were resolved on 6% polyacrylamide gels containing 7 M urea, and the conversion to product was measured with a Molecular Dynamics Phosphorimager and ImageQuant software. Reaction rates were obtained by plotting the fraction of substrate cleaved versus time and fitting the data to a single-exponential function (*5*):

$$[P]/[S]_{total} = A - Be^{-kt} \quad (2)$$

where [P] is the amount of product measured, $[S]_{total}$ is the total amount of substrate added to the reaction, A is the maximal extent of the reaction, B is the amplitude of the exponential, k is the observed cleavage rate, and t is the time of incubation. To calculate the cleavage rate at saturating enzyme concentrations, the rates determined from eq 2 were plotted as a function of the ribozyme concentration and the data were fit to (*30*)

$$k_{obs} = k_{app}/(1 + (K_m/[E])) \quad (3)$$

where k_{obs} is the cleavage rate obtained from eq 2 observed at enzyme concentration [E], k_{app} is the cleavage rate at saturating enzyme concentration, and K_m is equivalent to the Michaelis−Menten constant.

The dissociation constants for native and mutant RNase P RNAs were also determined by gel filtration as described previously (*5, 44*). Chromatography on Sephadex G-75 (Pharmacia) was used to measure the fraction of substrate bound to enzyme since free pre-tRNA can partition between the included and excluded volumes, while the enzyme−substrate complexes are excluded and so elute in the void volume. RNase P RNA and uniformly radiolabeled pre-tRNA were renatured separately in 1 M ammonium acetate, 50 mM Tris-HCl, pH 8.0, 25 mM calcium chloride, and 0.01% NP-40 by incubation at 65 °C for 90 s followed by incubation at 37 °C for 30 min. Ribozyme and substrate were combined and incubated together at 37 °C for 5 min before addition to disposable chromatography columns [Bio-Spin (Bio-Rad)] containing approximately 0.6 mL of packed G-75 resin equilibrated in 1 M ammonium acetate, 50 mM Tris-HCl, pH 8.0, 25 mM calcium chloride, and 0.01% NP-40. Columns were centrifuged for 2 min at 2500*g*. Ribozyme−substrate complexes in the flowthrough were recovered and the fraction of radiolabeled substrate bound was determined by Cerenkov counting. To determine K_d, the amount of bound substrate was plotted as a function of ribozyme concentration and the data were fit to a variation of eq 1:

$$[E-S]/[E-S]_\infty = 1/(1 + (K_d/[E])) \quad (1b)$$

where [E−S] is the amount of radioactivity recovered in the bound fraction, $[E-S]_\infty$ is the maximum amount of radioactivity recovered at the highest ribozyme concentrations, and [E] is the concentration of ribozyme in the binding reaction.

NAIM Analysis. For analysis of the positions of analogue incorporation, the bound and unbound RNAs were recovered by ethanol precipitation, washed with 70% ethanol, and resuspended at ca. 50 000 cpm/μL in 10 mM Tris-HCl, pH 8.0, and 0.5 mM EDTA. I_2 was used to cleave end-labeled RNAs at sites of phosphorothioate modification (*25*). Approximately 100 000 cpm of labeled RNA in 2 μL was combined with 2 μL of a 1:500 dilution in water of 0.1 M iodine in ethanol for a final concentration of 0.1 mM I_2. Following an incubation at 95 °C for 2 min, 4 μL of a solution containing 80% formamide, 0.05% bromophenol blue, and 0.05% xylene cyanol was added, and the 95 °C incubation was continued for an additional 2 min. A 1−2 μL aliquot of the sample was loaded on 6% or 10% denaturing acrylamide gels containing 7 M urea.

Intensities of bands corresponding to adenosine phosphorothioate (AαS) modification and nucleotide analogue (δαS) modification for each position in the bound and free populations were quantified with a Molecular Dynamics Phosphorimager and ImageQuant software. The extent of interference (I) for each position, normalized for phosphorothioate effects and variability in analogue incorporation, was calculated by using these values in (*26*)

$$I = \frac{(\delta\alpha S \text{ free}/\delta\alpha S \text{ bound})}{(A\alpha S \text{ free}/A\alpha S \text{ bound})} \quad (4)$$

The normalized interference values (κ) were obtained by dividing each individual interference value by the average interference value for each position within 2 standard deviations of the mean. This operation normalizes all interference data to a scale where $\kappa = 1$ indicates no interference, values greater than 1 indicate interference, and values lower than 1 indicate enhancement of activity due to analogue incorporation. The normalized interference values presented in Figure 5 and referred to in the text are averages from three independent experiments; standard errors were less than 30%. Because of this value, significant interferences referred to in the text were determined to give a κ value of 2 or greater. Due to almost complete loss of signal for the

strongest interferences, a value of 6 was set as the highest measurable κ value.

RESULTS AND DISCUSSION

Isolation of Ribozyme−Substrate Complexes. Detailed analysis of the ground-state binding interaction between RNase P RNA and pre-tRNA requires the ability to separate bound from unbound ribozyme prior to phosphodiester bond cleavage. For optimal folding and catalytic function, RNase P RNA utilizes magnesium; however, calcium can substitute for magnesium in the in vitro reaction. RNase P ribozymes folded in the presence of calcium have essentially the same three-dimensional structure as those folded in the presence of magnesium as assessed by intramolecular cross-linking (*21*−*23*, *32*). The ribozyme retains the ability to bind to substrate pre-tRNA with nearly the same K_d as in the presence of magnesium (*33*); importantly, however, the rate of pre-tRNA cleavage is significantly slower (ca. 10^4-fold).

To isolate enzyme−substrate complexes formed in the presence of calcium, we affinity-selected bound ribozyme on streptavidin−agarose beads by using a population of biotinylated substrates. Ribozyme was incubated together with biotinylated substrate pre-tRNA in solution, and ribozymes bound to substrate were separated from free ribozyme by incubation of the complexes with streptavidin−agarose beads followed by centrifugation. Figure 2A shows the recovery of radiolabeled RNase P RNA on streptavidin−agarose beads in the presence of either biotinylated or nonbiotinylated pre-tRNA. In this experiment, 25 nM radiolabeled *E. coli* RNase P RNA was incubated together with 400 nM biotinylated or nonbiotinylated pre-tRNA. This concentration of pre-tRNA was found to be saturating (see below; Figure 2B). After incubation at 37 °C for 5 min, the reaction was mixed with a small aliquot (30 μL) of streptavidin−agarose beads. The beads were recovered by a brief centrifugation and washed twice with binding reaction buffer, and the amount of radiolabeled ribozyme in the bound and free fractions was determined by Cerenkov counting. As anticipated, only a small fraction (<5%) of the radiolabeled RNase P RNA was recovered with the beads in the absence of pre-tRNA (data not shown) or when nonbiotinylated pre-tRNA was used (Figure 2A). In contrast, a significant fraction (ca. 50%) of the ribozyme was recovered with the beads when biotinylated pre-tRNA was used. These data indicate that ribozymes bound to pre-tRNA can be isolated from the free ribozyme population by virtue of their interaction with the biotinylated pre-tRNA substrate.

To characterize the interaction between RNase P RNA and biotinylated pre-tRNA, the amount of ribozyme recovered with the beads was determined as a function of biotinylated pre-tRNA concentration. Importantly, the fraction of biotinylated pre-tRNA recovered with the beads, approximately 80%, remains constant over a broad range of concentrations (1 nM−5 μM) (Figure 2B and data not shown). Figure 2B shows that increasing amounts of RNase P ribozyme are recovered in the bound fraction with increasing concentrations of biotinylated pre-tRNA. By fitting the data to a simple binding isotherm, an apparent K_d of 37 nM is obtained, which is in good agreement with the equilibrium binding constant for tRNA in the presence of calcium of 40 nM determined by gel-filtration chromatography as described in Materials and Methods (Table 1).

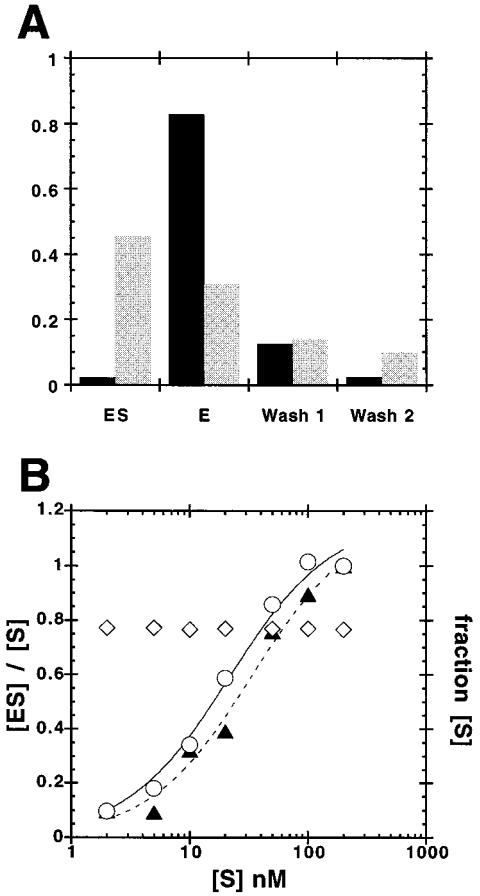

FIGURE 2: Binding of RNase P ribozyme to biotinylated pre-tRNA. (A) Recovery of P ribozyme on streptavidin−agarose beads in the presence of nonbiotinylated pre-tRNA (black columns) or biotinylated pre-tRNA (gray columns). The fraction of total radioactively labeled P ribozyme recovered in the bound (E−S), unbound (E), and wash fractions is shown. The biotinylated pre-tRNA concentration was 400 nM and radiolabeled ribozyme concentration was 25 nM. (B) Dependence of P ribozyme binding on pre-tRNA concentration. The fraction of the total radiolabeled pre-tRNA bound to streptavidin−agaroase beads at different concentrations of pre-tRNA is indicated by ◇. The fraction of radiolabeled RNase P RNA (○), or Ec165 RNA (▲) recovered with the streptavidin−agarose beads is shown as a function of pre-tRNA concentration. Lines represent a fit of the data to eq 1a.

Table 1: Kinetic Parameters for Native and Mutant *E. coli* RNase P Ribozymes

	K_d (nM) (gel filtration[a])	K_d (nM) (bio-pre-tRNA[a])	k_{app} (min^{-1}) (single turnover[b])
P RNA	39.8 ± 8.7	35.6 ± 6.0	1.9 ± 0.3
Ec165	52.2 ± 9.5	45.5 ± 2.9	2.5 ± 0.2
A136G	184.2 ± 42.8		1.5 ± 0.3
A132G	65.3 ± 7.8		2.3 ± 0.2

[a] 1 M ammonium acetate, 40 mM Tris-HCl, pH 8.0, and 25 mM $CaCl_2$. [b] 1 M ammonium acetate, 40 mM PIPES, pH 6.0, and 25 mM $MgCl_2$.

In addition, a circularly permuted RNase P RNA was also tested. Use of this ribozyme in subsequent interference analysis allowed mapping of 5′-end-labeled cleavage products close to the 3′ end of the native sequence (see below). The Ec165 circularly permuted RNase P RNA maintains the native *E. coli* RNase P RNA sequence but has the native 5′ and 3′ ends joined by a short oligonucleotide linker. The 5′ terminus of Ec165 RNA is located at G165, while the 3′

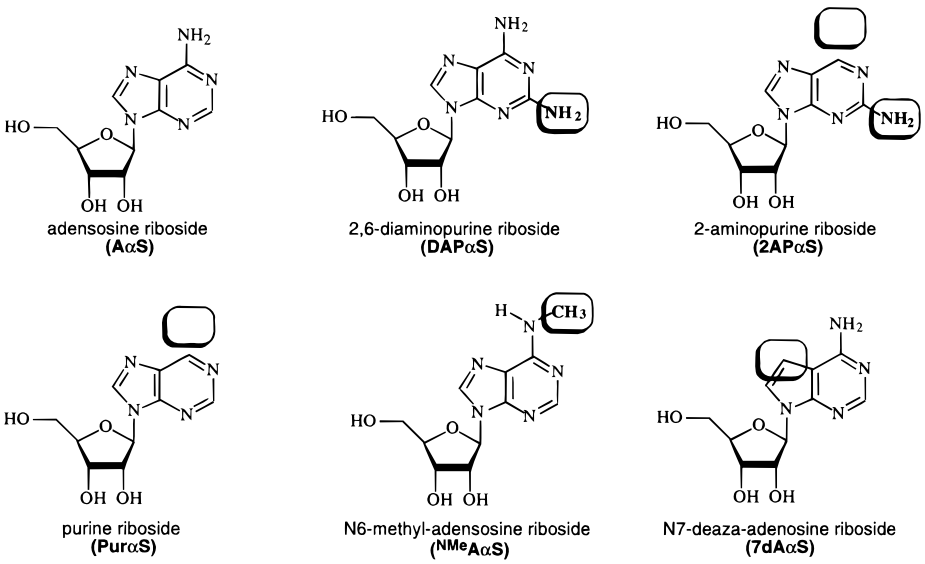

FIGURE 3: Adenosine nucleoside analogues used for interference mapping. Functional groups that are modified relative to adenosine are boxed. The abbreviations used in the text and in Figures 4 and 7 are shown in parentheses.

end is at G164. Figure 2B demonstrates that this ribozyme binds to the biotinylated substrate in a fashion nearly identical to the native ribozyme. For the Ec165 ribozyme, a K_d of 45 nM was measured for binding to the biotinylated substrate, while a value of 52 nM was measured by gel filtration (Table 1). Furthermore, cleavage of bound substrates by the Ec165 ribozyme occurred at a rate identical to that of the native ribozyme (ca. 2.2 min^{-1}) (Table 1). Taken together, these data indicate that few, if any, of the native binding contacts are disrupted in the complex of Ec165 and pre-tRNA. These data also demonstrate that both RNase P ribozymes bind to the biotinylated pre-tRNA substrate with an affinity that is essentially the same as for unmodified pre-tRNA.

The ability to separate ribozyme−substrate complexes allows NAIM to be used to identify ribozyme functional groups involved in substrate recognition. 5′-End-labeled ribozymes randomly substituted with a low level of phosphorothioate-tagged analogue were bound to the population of biotinylated substrates, and the ribozymes competent to bind substrate were isolated by their association with the agarose beads. Bound (E−S) and free ribozymes (E) were recovered and cleaved with iodine at positions of analogue incorporation (*25*). Comparison of the patterns of chemical modification in the E−S and E fractions reveals those nucleotides that, when modified, interfere with the ability of the ribozyme to bind substrate. To identify potential contact points with the substrate, the binding reactions were carried out at high (1 M) monovalent salt concentrations, which can suppress kinetic defects due to structural distortion (*21*, *32*, *34*).

For initial analysis of ribozyme functional groups, we employed the series of adenosine analogues shown in Figure 3. This collection of reagents is useful for surveying the maximal number of conserved RNase P nucleotides; almost 40% (24 out of 61) of the conserved nucleotides in RNase P RNA are adenosine. Also, these analogues identify interference effects due to modification in both the major- and minor-groove faces of the adenine base. Three analogues probe the N6 position: ^{NMe}AαS, 2APαS, and PurαS. PurαS and 2APαS both lack the adenosine N6 amine, while ^{NMe}AαS has one of the N6 amine hydrogens replaced by a methyl group. DAPαS and 2APαS have an additional amine group at the 2-position of the purine ring and so examine the tolerance of an additional functional group on the minor-groove edge of the base. The N2 exocyclic amine is only present on G; thus, sensitivity to these reagents identifies positions where an A to G mutation could disrupt function by addition of an N2 amine. 7dAαS has a carbon atom in place of N7 and thus eliminates a potential hydrogen-bond acceptor in the major groove. Previously, it has been shown that these analogues are all incorporated accurately and efficiently into the group I ribozyme from *Tetrahymena* (*26*). Iodine cleavage of 5′-end-labeled RNA demonstrates that these analogues are also incorporated exclusively at A positions in both the *E. coli* and *B. subtilis* RNase P ribozymes (Figures 4 and 7 and data not shown).

Nucleotide Base Functional Groups in Helix P4 Are Important for both Substrate Binding and Catalysis. Helix P4 is a core element of secondary structure that includes several universally conserved nucleotides. Chemical modification of backbone positions in P4, including A67, G68, U69, and A351, disrupts both substrate binding and catalytic function (*28*, *29*, *36*). Consistent with the previous analyses, we detect a strong phosphorothioate interference 5′ to A67 (Figure 4A). Because all of the analogues used in this study are phosphorothioate derivatives, interference is also detected at A67 with all five of the analogues. In contrast, interferences at A65 and A66 detected with the analogue phosphorothioates are attributed solely to analogue-specific functional group modification. To quantify individual interference effects, the results were normalized to the phosphorothioate interference effect for each position, as well as for differences in analogue incorporation as described in Materials and Methods. The resulting normalized interference value (κ) for each adenosine position in the *E. coli* RNase P RNA ribozyme is reported in Figure 5. A value of 1 indicates no interference, while values greater than 1 reflect interference due to analogue incorporation.

Interestingly, differences in the pattern of analogue sensitivity are detected at the adjacent conserved adenosines A65 and A66 in helix P4. Incorporation of DAPαS does not result in interference at A66 or A65, indicating that both

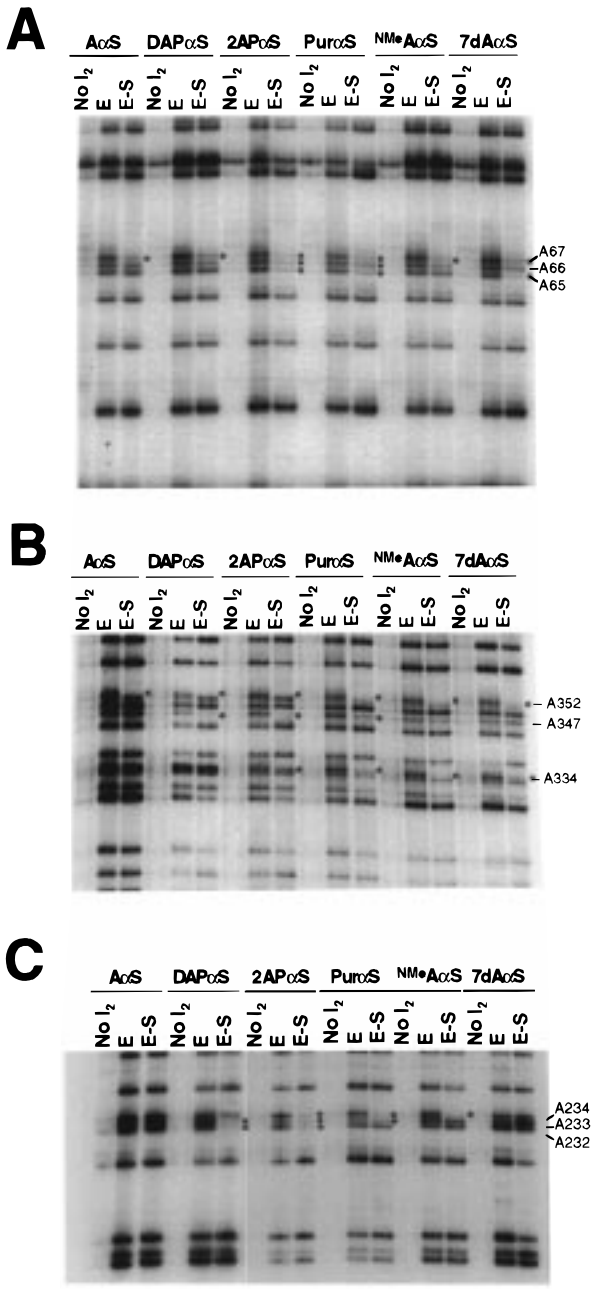

FIGURE 4: Analogue interference mapping using native *E. coli* RNase P RNA and Ec165 RNA. Positions of analogue incorporation were detected by iodine cleavage. Lanes marked No I_2 are free enzyme samples that were not cleaved by iodine. Lanes labeled E represent the iodine cleavage products from the free enzyme population, and lanes marked E−S represent the products from the bound fraction. The identity of the analogue incorporated for each RNA is indicated with the abbreviations shown in Figure 2. Sites of analogue interference are indicated by asterisks. The corresponding nucleotide position in the *E. coli* ribozyme is shown at right. (A) 5′ portion of the P4 helix, nucleotides 49−89. (B) Interference pattern in P18, J18/2, P2, and J2/4, nucleotides 320−368. (C) Interference pattern in P11, nucleotides 214−245.

nucleotides can accommodate an additional amine in the minor groove at the 2-position. In contrast, both A65 and A66 are highly sensitive ($\kappa \geq 4$) to substitution with 2APαS and PurαS, demonstrating that removal of the N6 amine on the major-groove edge of either A66 or A65 interferes strongly with substrate binding. These two N6 amines are not functionally equivalent, however, since methylation of the N6 amine on A66 results in interference ($\kappa \approx 2.5$), whereas the same modification at A65 does not (Figures 4A and 5). The roles of these two conserved nucleotides are further distinguished by their differential sensitivity to 7dAαS. A significant level of sensitivity is detected for incorporation of 7dAαS at A65 ($\kappa = 6$), while A66 is less sensitive to this reagent ($\kappa \approx 2$).

Previously, Kazantsev and Pace detected 7dAαS interference at A65 in P4 by using self-cleavage of a tethered ribozyme-substrate conjugate for interference analysis (*35*). In their analysis, the interference effect at A65 was ameliorated when the self-cleavage selection was performed under conditions where phosphodiester bond cleavage was rate-limiting. This suggests that the interference effect was manifested at a step in the RNase P RNA-catalyzed cleavage reaction distinct from phosphodiester bond hydrolysis. Our observation that the 7dAαS incorporation at A65 interferes with ground-state substrate binding is consistent with the hypothesis that N7 of A65 functions at an early step in the reaction pathway, such as formation of an interaction with the substrate.

These results demonstrate involvement of P4 base functional groups in substrate binding, highlighting the importance of this universally conserved structural element. The lack of sensitivity to DAPαS at A66, in contrast to the sensitivity of this nucleotide to deletion or modification of the N6 amine, is consistent with previous arguments that the major groove of P4 is the functionally relevant portion of this helix (*36*). This idea is further supported by the cluster of phosphate oxygens that are important for both substrate binding and catalysis at the base of P4, since these groups face the major-groove side of A-form RNA helices. The clustering of conserved nucleotides, as well as backbone and base functional groups important for both substrate binding and catalysis, is consistent with the proposal that helix P4 forms a portion of the active site of RNase P RNA (*36*, *37*, *38*).

Figure 4B shows the interference pattern in J2/4, which forms a long junction between P1−3 and P4; the specific role of this element of RNase P RNA structure is only poorly defined. A strong phosphorothioate interference effect, also detected in previous interference analyses (*28*, *36*), is observed at position A351. Although J2/4 contains several universally conserved adenosines, only A347 displays sensitivity to analogue substitution. DAPαS interferes at this position; thus introduction of an N2 amine has a detrimental effect on binding. In addition, A347 is sensitive to PurαS, indicating that deletion of the N6 amine interferes with function. 2APαS, as expected, also gives rise to interference at A347, based on the presence of both deleterious modifications: an additional N2 amine and deletion of the N6 amine. Neither ^{NMe}AαS nor 7dAαS interferes strongly at this position. Recently, Westhof and colleagues have argued on the basis of structural considerations that J2/4 is in close proximity to the pre-tRNA substrate (*39*). Our observation that functional groups on a universally conserved nucelotide in J2/4 are involved in substrate binding is consistent with this idea; however, the precise interactions between J2/4 and the substrate require further investigation.

Identification of Conserved Adenosines Important for Substrate Binding in J5/15 and J18/2. J5/15 and J18/2 are located in proximity to the base of the acceptor stem of the pre-tRNA substrate (Figure 6) (*18*, *20*−*22*, *44*) and thus are

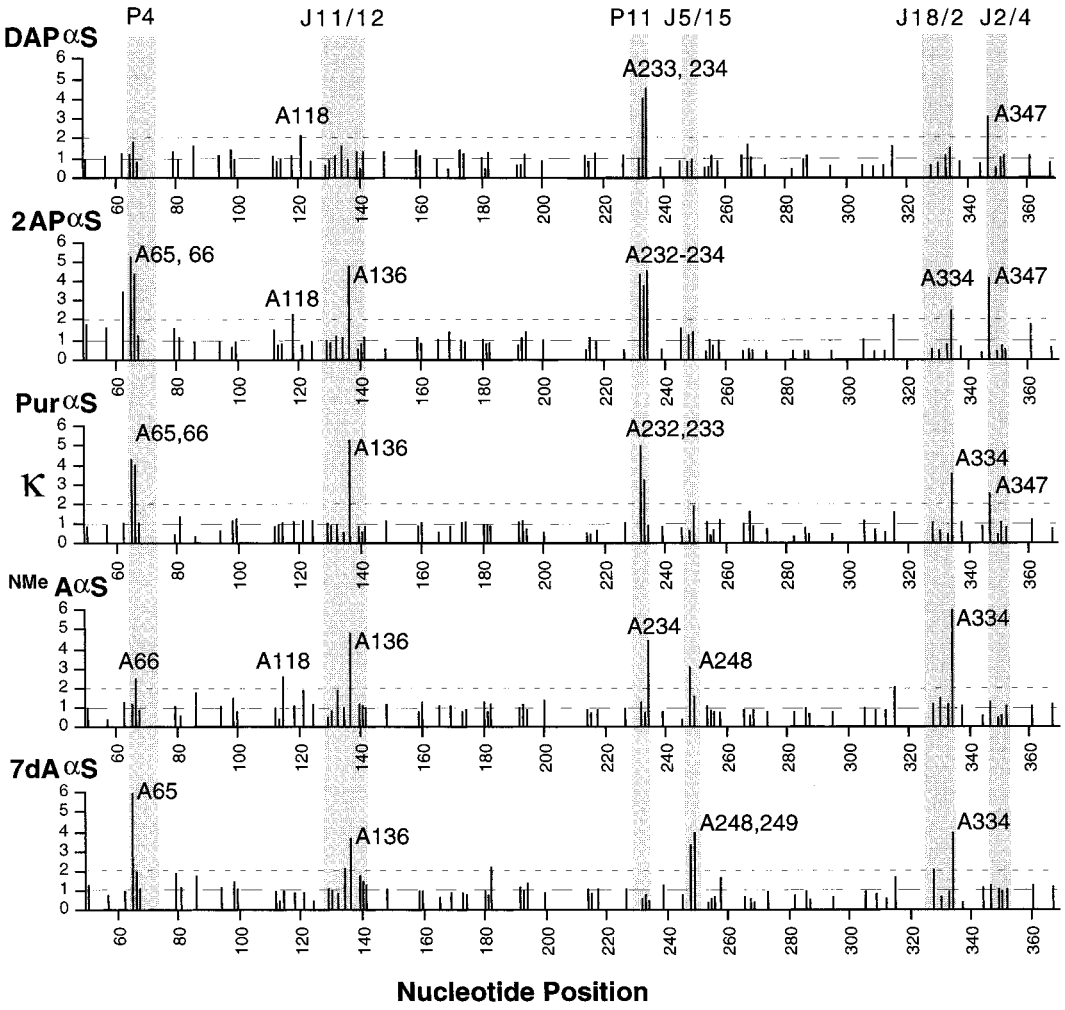

FIGURE 5: Quantification of NAIM results. Interference effects were quantified as described in Materials and Methods. The normalized interference value (κ) for each adenosine position is shown as a vertical line with length proportional to κ. Nucleotide positions with normalized interference values greater than 2 are indicated. The corresponding regions of the RNase P ribozyme secondary structure where the sensitive positions are located are indicated by gray boxes.

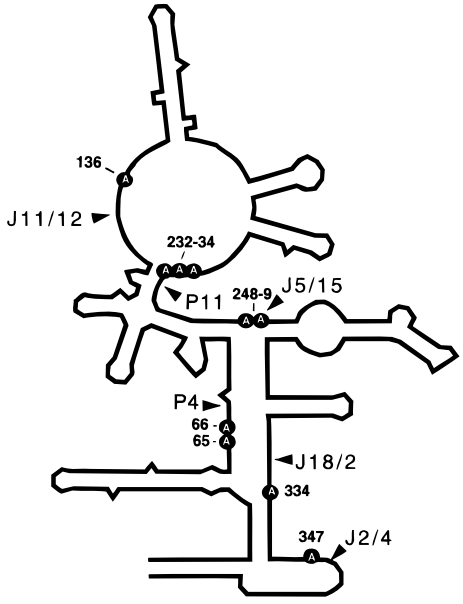

FIGURE 6: Location of sensitive nucleotides in *E. coli* RNase P RNA. In the secondary structure diagram of *E. coli* RNase P RNA, adenosine positions sensitive to analogue incorporation are indicated by black circles. The regions of RNase P secondary structure referred to in the text are indicated by arrows.

likely candidates for elements directly involved in substrate recognition. However, the individual nucleotides within these elements that are important for enzyme function are undefined. We find that conserved adenosines at positions A248 and A249 in J5/15 and A334 in J18/2 are sensitive to base analogue substitution, consistent with a direct role in ribozyme−substrate interactions.

A328, A330, and A334 in J18/2 are highly conserved; however, we detect significant interference only at A334 with this set of analogues (Figures 4B and 5). A334 is sensitive to both deletion and methylation of the N6 amine, as 2APαS, PurαS, and ^{NMe}AαS all result in measurable interference ($\kappa > 2$) at this position. Additionally, A334 is sensitive to 7dAαS incorporation. The sensitivity of A334 to modification of the N6 and N7 positions, both of which lie on the major-groove edge of the purine base, implies that this adenosine may participate in a Hoogsteen-type hydrogen-bonding interaction. Hartmann and co-workers found that mutation of A334 to U results in a ca. 50-fold increase in the equilibrium binding constant for pre-tRNA, consistent with alteration of multiple essential functional groups on this nucleotide (*40*). Interestingly, despite the fact that they are universally conserved, mutations at A328 and A330 had significantly less effect on in vitro reaction kinetics than

mutations at A334 (*40*), consistent with the relative insensitivity of A328 and A330 to analogue incorporation relative to A334.

J5/15 is in proximity to both J18/2 and the base of the tRNA acceptor stem in the ribozyme−substrate complex (*20, 21, 32*). Both conserved adenosines A248 and A249 in J5/15 show significant interference with 7dAαS ($\kappa > 2$), and A248 is also sensitive to ^{NMe}AαS ($\kappa > 2$) (Figure 5). 7dAαS at both A248 and A249 also interferes with self-cleavage of a ribozyme−substrate tether, but these effects are rescued by lowering the pH or by increasing the magnesium ion concentration, arguing against a direct role in catalysis (*35*; Kaye and Harris, unpublished results). Recently, we detected efficient short-range (1−2 Å) cross-linking between position G + 1 in tRNA and A248 in the ribozyme (*44*). The close proximity of A248 and the conserved tRNA position +1 and the sensitivity to ^{NMe}AαS and 7dAαS interference argues strongly that the major-groove edge of A248 plays a direct role in substrate recognition.

Identification of Essential Ribozyme Functional Groups in P11 Adjacent to the tRNA T-Stem Loop in the Ribozyme−Substrate Complex. One region of tRNA that is in direct contact with the ribozyme through a series of functional groups is the T-stem loop (*15, 16*). Mutational and in vitro kinetic studies implicated *B. subtilis* RNase P RNA nucleotides A230 and A130 in this interaction (*16*). The mutational data and the modification experiments have not been recapitulated in *E. coli* RNase P RNA in order to confirm that these interactions are general. However, both of the nucleotides homologous to A230 and A130 in *E. coli* (A233 and A118, respectively) are protected from chemical modification of N1 in the presence of substrate in both RNAs (*18*), and photo-cross-linking confirms the proximity of P11 and P9 nucleotides to the T-stem loop (*23*).

We find that A118 in P9 shows measurable, but low, sensitivity to modification of the N6 amine. Methylation of N6 interferes only weakly with the function of A118 in substrate binding ($\kappa \approx 2.5$). Also, this position is somewhat sensitive to introduction of an N2 amine since both 2APαS and DAPαS give rise to small ($\kappa \approx 2$) effects at A118 (Figure 5). In contrast to the relatively weak interferences at A118, we detect a cluster of strong interferences at positions A232−234 in the *E. coli* ribozyme, which are homologous to the sites of interaction with the T-stem loop in *B. subtilis* RNase P RNA (Figures 4C and 5). Remarkably, the sensitivity of these three adjacent nucleotide positions to analogue incorporation is quite distinct. Function at A232 and A233 is disrupted by addition of an extra amine at position 2 since both are strongly sensitive to DAPαS ($\kappa \geq 3$). A233 and A234 require N6, as indicated by their sensitivity to PurαS ($\kappa \geq 3$). All three positions are dominantly sensitive to 2APαS as expected due to their sensitivities to the PurαS and DAPαS reagents ($\kappa \approx 5$). A233 cannot accommodate an additional N2 amine, as demonstrated by its sensitivity to both 2APαS and DAPαS. However, A234 is sensitive to 2APαS solely because of the missing N6 group since this nucleotide is insensitive to DAPαS, which has amines at both N6 and N2; while PurαS, which is missing the N6 amine, does interfere. A234 does not tolerate methylation of N6 as indicated by sensitivity to ^{NMe}AαS; however, neither A233 nor A234 is sensitive to this analogue. In summary, these data show that functional groups on both the major- and minor-groove edges of A233 affect its function, while only the minor groove of A232 and only the major groove of A234 are sensitive to functional group modification.

Given that the homologue of A233 in *B. subtilis* has been demonstrated to interact with a 2′ hydroxyl at the top of the T-stem [position 60 (*15*)], it seems likely that the interference effects we detect also disrupt this interaction. Intriguingly, mutation of the A233 homologue to G in the *B. subtilis* ribozyme results in a very large increase in the K_d for substrate binding (ca. 50-fold). Our results suggest that the large effect of this mutation is due to both introduction of an N2 amine and changing the N6 position from an amine, in adenosine, to the carbonyl found on the guanosine base.

Interestingly, A234 is one of only two paired adenosine positions we detect as sensitive to analogue substitution (the second is A66 in helix P4; Figures 4A and 6). Phylogenetic comparative analysis indicated that nucleotides homologous to A234 covary with U126; however, the vast majority of nucleotides in this position result in a U-A pair, which occurs 121 out of 141 times. G-C occurs at this position 11 times, and the other four possible base-pairing configurations occur a total of only nine times combined (*41*). Therefore, the sensitivity of A234 to analogues that delete the N6 amine (PurαS and 2APαS) correlates well with phylogenetic conservation of a major-groove amine that would be present on both the U-A and G-C pairings predominantly found at this position. Introduction of an N2 amine into this U−A pair is not expected to significantly disrupt Watson−Crick interactions. In fact, DAP might lead to incremental stabilization of helixes due to a potential hydrogen-bonding interaction between the N2 amine of DAP and the O2 moiety of the uridine base; thus it is not surprising that we do not detect sensitivity of A234 to DAPαS.

Comparative Interference and Mutational Analysis Implicates the Involvement of a Universally Conserved J11/12 Nucleotide in Substrate Binding. J11/12 contains nucleotides conserved not only among bacterial RNase P RNAs but also among RNAs from all three phylogenetic domains (*1, 43*). This region of yeast RNase P RNA has been proposed to bind divalent metal ions essential for enzyme function (*42*); however, the role of J11/12 in bacterial RNase P RNAs remains largely unexplored. Intriguingly, we detect A136, a universally conserved adenosine nucleotide that has not yet been found to play a role in substrate binding, to be sensitive to analogue substitution (Figures 5 and 7A). A136 is dominantly sensitive to both 2APαS and PurαS substitution ($\kappa \approx 6$) indicating the N6 amine here is essential. Methylation of this group is also quite detrimental to function, as is substitution at the N7 nitrogen, since ^{NMe}AαS ($\kappa \approx 5$) and 7dAαS ($\kappa \approx 3$) both interfere at A136. This pattern of sensitivity to reagents that modify N7 and the N6 amine but insensitivity to introduction of an amine at N2 is consistent with a Hoogsteen-type hydrogen-bonding interaction involving A136.

The interference at A136 was unanticipated, since no previous cross-linking, mutational, or interference studies had identified this region as being involved in substrate binding, or being in contact with the pre-tRNA substrate. To test the generality of this interference result, as well as the interference method in general, we repeated the analysis of J11/12 using the *B. subtilis* ribozyme (Figure 7B). The RNase P RNA from *B. subtilis* differs significantly in details of

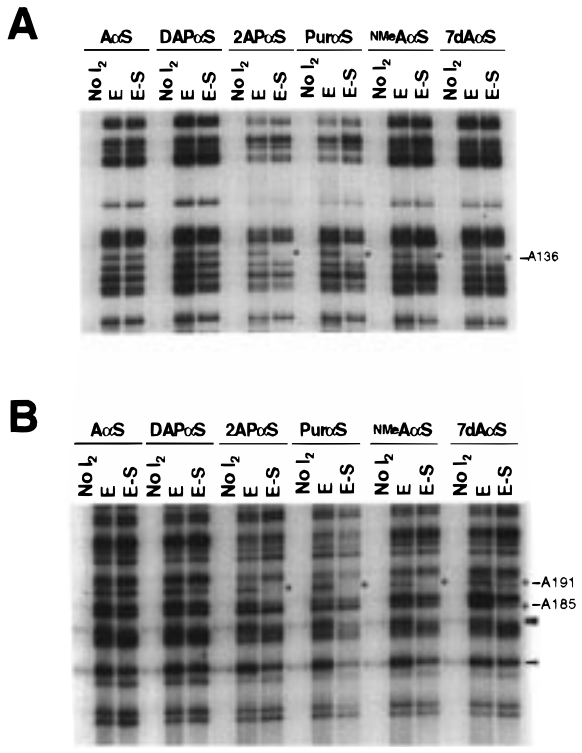

FIGURE 7: Analogue interference analysis of J11/12 in *E. coli* and *B. subtilis* RNase P RNAs. (A) NAIM results for the *E. coli* ribozyme. Lanes are marked as in Figure 3. Sites of analogue interference are indicated by asterisks. (B) NAIM results for J11/12 in the *B. subtilis* ribozyme. Lanes and sensitive nucleotide positions are marked as in panel A.

secondary structure from *E. coli* RNase P RNA, but it retains the same core of conserved sequence and structure found in all bacterial RNase P RNAs. Overall, the interference pattern obtained with this ribozyme was essentially the same as that obtained with the *E. coli* ribozyme (Figure 7B; data not shown). Importantly, we find that the homologue of *E. coli* A136 in *B. subtilis* (A191) shows an identical pattern of analogue interference. That is, *B. subtilis* A191 is sensitive to 2APαS, PurαS, ^{NMe}AαS, and 7dAαS but insensitive to DAPαS. Although we detect nearly identical patterns of analogue interference in both *E. coli* and *B. subtilis*, some ribozyme-specific interferences are seen. One example, located in J11/12, is seen in Figure 7B, where 7dAαS gives rise to a strong interference effect at A185 while *E. coli* RNase P RNA has a C at this position. Such differences are likely to reflect differences in structure, yet it is not possible to discount the possibility that differences in specific ribozyme−substrate interactions may exist between these two ribozymes. The basis for these differences is currently being explored.

To further examine the general sensitivity to analogue interference at A136, the binding properties of a mutation at A136 was explored along with a similar mutation at a nearby conserved adenosine that is not sensitive to analogue interference. Mutation of A136 to G alters three different positions on the purine base: N1, N2, and N6. On the basis of the interference results, addition of N2 should not disrupt the function of A136 since this position is not sensitive to DAPαS. However, G replaces the exocyclic amine of A with a carbonyl at position 6, which changes the chemical nature of this position. Such a change would be expected to significantly affect substrate binding since deletion or modification of N6 strongly interferes in both ribozymes tested. In addition, N1 of the purine ring is protonated in G relative to A; however, none of the analogues tested were modified at this position.

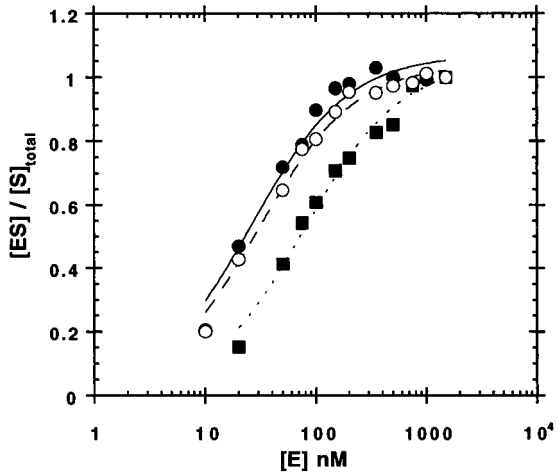

FIGURE 8: Analysis of A132G and A136G mutants of *E. coli* RNase P RNA. Bound and unbound substrate were separated by gel-filtration chromatography and the fraction of substrate bound was plotted as a function of ribozyme concentration. Native *E. coli* ribozyme (●); A132G (○), and A136G (■) are shown. Lines represent a fit of the data to eq 1b.

As expected on the basis of the interference results, mutation of A136 to G gives rise to a measurable (ca. 5-fold) increase in K_d for pre-tRNA binding compared to the wild-type ribozyme (Figure 8, Table 1). Using the gel-filtration approach described above, we measure a K_d for pre-tRNA of 40 nM for the native RNase P RNA, while a value of 184 nM is obtained for the A136G mutant ribozyme. Interestingly, an analogous mutation to guanosine at A132, which is not sensitive to analogue interference in either ribozyme, has little effect on the ability of the ribozyme to bind substrate. For the A132G mutant a value of 65 nM is measured for K_d, which is less than 2-fold higher than the value measured for the native ribozyme. Importantly, neither mutation has a significant effect on the ability of the ribozyme to cleave the bound substrate since the single-turnover cleavage rate is essentially unaffected (Figure 8, Table 1).

CONCLUSIONS

These results provide a detailed chemical picture of ribozyme functional groups that are involved in substrate binding. We detect 10 adenosine residues out of 86 in *E. coli* RNase P RNA (12%) that are sensitive to at least one of the base analogues tested: A65, A66, A136, A232−234, A248, A249, A334, and A347. All of the interfering positions are located at nucleotides that are highly conserved among bacterial RNase P RNAs. In fact, the majority of the interfering sites (7 out of 10; A65, A66, A136, A248, A249, A334, and A347) are located at nucleotides that are universally conserved among RNase P RNAs from all three phylogenetic domains (*1*, *43*). Notably, we observe a strong correlation between nucleotide positions that are sensitive to analogue interference in substrate binding and sites identified by photo-cross-linking and chemical protection as being involved in ribozyme−substrate interactions. In ad-

dition, these results have identified another specific region of the ribozyme, J11/12, that is involved in substrate recognition. A subset of the conserved nucleotides we detect likely form direct contacts with the substrate. These results represent a crucial step toward defining the role of these conserved nucleotides in ribozyme function. With the important functional groups established, their tertiary pairing partners can likely be elucidated by kinetic analysis and interference suppression approaches (e.g., ref *27*). Given that nearly all of the functional groups we detect reside at universally conserved nucleotide positions, it is likely that the results will be useful for understanding the function of RNase P RNAs from all three phylogenetic domains.

ACKNOWLEDGMENT

We thank Dr. James Bruzik for assistance in applying the biotin−streptavidin selection procedure and generous gifts of materials and reagents in the initial stages of this study. Also, we thank Dr. Eric Christian, Nick Kaye, Dr. Jonatha Gott, Dr. JoAnn Wise, Dr. Timothy Nilsen, and Frank Campbell for advice and critical review of the manuscript.

REFERENCES

1. Chen, J. L., and Pace, N. R. (1997) *RNA 3*, 557−560.
2. Brown, J. W. (1998) *Nucleic Acids Res. 26*, 351−352.
3. Guerrier-Takada, C., Gardiner, K., Marsh, T., Pace, N., and Altman, S. (1983) *Cell 35*, 849−857.
4. Harris, M. E., Frank, D. F., and Pace, N. R. (1997) in *RNA Structure and Function* (Simons, R. W., and Grunberg-Manago, M., Eds.) pp 309−337, Cold Spring Harbor Laboratory Press, Plainview, NY.
5. Beebe, J. A., and Fierke, C. A. (1994) *Biochemistry 33*, 10294−10304.
6. Hardt, W. D., Schlegl, J., Erdmann, V. A., and Hartmann, R. K. (1993) *Nucleic Acids Res. 21*, 3521−3527.
7. McClain, W. H., Guerrier-Takada, C., and Altman, S. (1987) *Science 238*, 527−530.
8. Thurlow, D. L., Shilowski, D., and Marsh, T. L. (1991) *Nucleic Acids Res. 19*, 885−891.
9. Kahle, D., Wehmeyer, U., and Krupp, G. (1990) *EMBO J. 9*, 1929−1937.
10. Kirsebom, L. A., and Svard, S. G. (1994) *EMBO J. 13*, 4870−4876.
11. Loria, A., and Pan, T. (1998) *Biochemistry 37*, 10126−10133.
12. Gaur, R. K., and Krupp, G. (1993) *Nucleic Acids Res. 21*, 21−26.
13. Kahle, D., Kust, B., and Krupp, G. (1993) *Biochimie 75*, 955−962.
14. Hardt, W. D., Schlegl, J., Erdmann, V. A., and Hartmann, R. K. (1993) *Biochemistry 32*, 13046−13053.
15. Pan, T., Loria, A., and Zhong, K. (1995) *Proc. Natl. Acad. Sci. U.S.A. 92*, 12510−12514.
16. Loria, A., and Pan, T. (1997) *Biochemistry 36*, 6317−6325.
17. Haas, E. S., Brown, J. W., Pitulle, C., and Pace, N. R. (1994) *Proc. Natl. Acad. Sci. U.S.A. 91*, 2527−2531.
18. LaGrandeur, T. E., Huttenhofer, A., Noller, H. F., and Pace, N. R. (1994) *EMBO J. 13*, 3945−3952.
19. Oh, B.-K., and Pace, N. R. (1994) *Nucleic Acids Res. 22*, 4087−4094.
20. Burgin, A. B., and Pace, N. R. (1990) *EMBO J. 9*, 4111−4118.
21. Harris, M. E., Nolan, J. M., Malhotra, A., Brown, J. W., Harvey, S. C., and Pace, N. R. (1994) *EMBO J. 13*, 3953−3963.
22. Harris, M. E., Kazantsev, A. V., Chen, J.-L., and Pace, N. R. (1997) *RNA 3*, 561−576.
23. Nolan, J. M., Burke, D. H., and Pace, N. R. (1993) *Science 261*, 762−765.
24. Strobel, S. A., and Shetty, K. (1997) *Proc. Natl. Acad. Sci. U.S.A. 94*, 2903−2908.
25. Gish, G., and Eckstein, F. (1988) *Science 240*, 1520−1522.
26. Ortoleva-Donnelly, L., Szewczak, A. A., Gutell, R. R., and Strobel, S. A. (1998) *RNA 4*, 498−519.
27. Strobel, S. A., Ortoleva-Donnelly, L., Ryder, S. P., Cate, J. H., and Moncoeur, E. (1998) *Nat. Struct. Biol. 5*, 60−66.
28. Hardt, W. D., Warnecke, J. M., Erdmann, V. A., and Hartmann, R. K. (1995) *EMBO J. 14*, 2935−2944.
29. Hardt, W. D., Erdmann, V. A., and Hartmann, R. K. (1996) *RNA 2*, 1189−1198.
30. Fersht, A. R. (1985) *Enzyme Structure and Mechanism*, Freeman, New York.
31. Smith, D., and Pace, N. R. (1993) *Biochemistry 32*, 5273−5281.
32. Chen, J.-L., Nolan, J. M., Harris, M. E., and Pace, N. R. (1998) *EMBO J. 17*, 1515−1525.
33. Smith, D., Burgin, A. B., Haas, E. S., and Pace, N. R. (1992) *J. Biol. Chem. 267*, 2429−2436.
34. Darr, S. C., Zito, K., Smith, D., and Pace, N. R. (1992) *Biochemistry 31*, 328−333.
35. Kazantsev, A. V., and Pace, N. R. (1998) *RNA 4*, 937−947.
36. Harris, M. E., and Pace, N. R. (1995) *RNA 1*, 210−218.
37. Frank, D. N., and Pace, N. R. (1997) *Proc. Natl. Acad. Sci. U.S.A. 94*, 14355−14360.
38. Frank, D. N., Ellington, A. E., and Pace, N. R. (1996) *RNA 2*, 1179−1188.
39. Massire, C., Jaeger, L., and Westhof, E. (1998) *J. Mol. Biol. 279*, 773−793
40. Schlegl, J., Hardt W. D., Erdmann, V, A., and Hartmann, R. K. (1994) *EMBO J. 13*, 4863−4869.
41. Brown, J. W. (1998) *Nucleic Acids Res. 26*, 351−352.
42. Ziehler, W. A., Yang, J., Kurochkin, A. V., Sandusky, P. O., Zuiderweg, E. R., and Engelke, D. R. (1998) *Biochemistry 37*, 3549−3557.
43. Pitulle, C., Garcia-Paris, M., Zamudio, K. R., and Pace, N. R. (1998) *Nucleic Acids Res. 26*, 3333−3339.
44. Christian, E. L., McPheeters, D. S., and Harris, M. E. (1998) *Biochemistry 37*, 17618−17628.

BI982329R